

Accelerated Articles**Chromogenic Cross-Linker for the Characterization of Protein Structure by Infrared Multiphoton Dissociation Mass Spectrometry**

Myles W. Gardner, Lisa A. Vasicek, Shagufta Shabbir, Eric V. Anslyn, and Jennifer S. Brodbelt*

Department of Chemistry and Biochemistry, The University of Texas at Austin, 1 University Station A5300, Austin, Texas, USA 78712

We have developed a new IR chromogenic cross-linker (IRCX) to aid in rapidly distinguishing cross-linked peptides from unmodified species in complex mixtures. By incorporating a phosphate functional group into the cross-linker, one can take advantage of its unique IR absorption properties, affording selective infrared multiphoton dissociation (IRMPD) of the cross-linked peptides. In a mock mixture of unmodified peptides and IRCX-cross-linked peptides (intramolecularly and intermolecularly cross-linked), only the peptides containing the IRCX modification were shown to dissociate upon exposure to 50 ms of 10.6- μm radiation. LC-IRMPD-MS proved to be an effective method to distinguish the cross-linked peptides in a tryptic digest of IRCX-cross-linked ubiquitin. A total of four intermolecular cross-links and two dead-end modifications were identified using IRCX and LC-IRMPD-MS. IRMPD of these cross-linked peptides resulted in secondary dissociation of all primary fragment ions containing the chromophore, producing a series of unmodified b- or y-type ions that allowed the cross-linked peptides to be sequenced without the need for collision-induced dissociation.

As the field of proteomics continues to rapidly expand, there has been a growing interest in determining the three-dimensional structure of proteins as well as the interfaces of protein–protein complexes.^{1,2} Chemical cross-linking of proteins with mass spectrometric analysis has proven to be a useful method to determine low-resolution protein structural information and

protein–protein interactions.^{3–6} Compared to X-ray crystallography and NMR spectroscopy, chemical cross-linking requires relatively low amounts of protein to probe distance constraints within a single protein⁷ or protein–ligand complexes.^{8–10} While the experimental procedure for chemically cross-linking proteins is well established, there are several analytical challenges that remain in the identification of the cross-linked peptides by mass spectrometric means. The two main difficulties in this technique have been the differentiation of cross-linked peptides from unmodified ones in enzymatic digests of cross-linked proteins and the ability to identify the specific location of the cross-link using tandem MS.

To circumvent these limitations, much work has been dedicated to developing new cross-linkers to simplify identification by mass spectrometric methods. For example, several cross-linkers that incorporate isotope labels have been designed to create doublet peaks within the mass spectra,^{11–14} thus allowing facile pinpointing of the cross-linked products. Other cross-linkers

- (3) Back, J. W.; De Jong, L.; Muijsers, A. O.; De Koster, C. G. *J. Mol. Biol.* **2003**, *331*, 303–313.
- (4) Sinz, A. *Mass Spectrom. Rev.* **2006**, *25*, 663–682.
- (5) Sinz, A. *J. Mass Spectrom.* **2003**, *38*, 1225–1237.
- (6) Young, M. M.; Tang, N.; Hempel, J. C.; Oshiro, C. M.; Taylor, E. W.; Kuntz, I. D.; Gibson, B. W.; Dollinger, G. *Proc. Natl. Acad. Sci. U. S. A.* **2000**, *97*, 5802–5806.
- (7) Huang, B. X.; Kim, H.-Y.; Dass, C. *J. Am. Soc. Mass Spectrom.* **2004**, *15*, 1237–1247.
- (8) Carlsohn, E.; Angstrom, J.; Emmett, M. R.; Marshall, A. G.; Nilsson, C. L. *Int. J. Mass Spectrom.* **2004**, *234*, 137–144.
- (9) Lanman, J.; Lam, T. T.; Barnes, S.; Sakalian, M.; Emmett, M. R.; Marshall, A. G.; Prevelige, P. E. *J. Mol. Biol.* **2003**, *325*, 759–772.
- (10) Back, J. W.; Sanz, M. A.; De Jong, L.; De Koning, L. J.; Nijtmans, L. G. J.; De Koster, C. G.; Grivell, L. A.; Van Der Spek, H.; Muijsers, A. O. *Protein Sci.* **2002**, *11*, 2471–2478.
- (11) Mueller, D. R.; Schindler, P.; Towbin, H.; Wirth, U.; Voshol, H.; Hoving, S.; Steinmetz, M. O. *Anal. Chem.* **2001**, *73*, 1927–1934.
- (12) Back, J. W.; Notenboom, V.; de Koning, L. J.; Muijsers, A. O.; Sixma, T. K.; de Koster, C. G.; de Jong, L. *Anal. Chem.* **2002**, *74*, 4417–4422.

* To whom correspondence should be addressed. E-mail: jbrodbelt@mail.utexas.edu.

- (1) Borch, J.; Jorgensen, T. J. D.; Roepstorff, P. *Curr. Opin. Chem. Biol.* **2005**, *9*, 509–516.
- (2) Heck, A. J. R.; van den Heuvel, R. H. H. *Mass Spectrom. Rev.* **2004**, *23*, 368–389.

incorporate fluorophores to facilitate distinction of modified proteins¹⁵ and peptides from the unmodified ones during LC–MS analyses,^{16,17} while others introduce chemically cleavable functionalities.^{18–20} Affinity tags such as biotin labels have also shown promise as a means to enrich the cross-linked peptides from complex mixtures prior to mass spectrometry.^{20–22} Cross-linkers have also been designed with gas-phase labile bonds such that traceable fragment ions unique to cross-linked peptides are formed upon low-energy activation during MS/MS analysis.^{20,23–25}

Interpretation of the cross-linked peptide product ion spectra, which typically contain diagnostic fragment ions both to locate the cross-link and to sequence the peptides, remains a difficult challenge even with available software. Several algorithms have been written to aid in the identification of intact cross-linked peptides based on product ion spectra of these species, but they do not take into account all of the possible product ions specific to cross-linked peptides.^{26–31} Initial work by Schilling et al. demonstrated that dissociation of cross-linked peptides typically resulted in cleavage of an amide bond of one peptide, yielding one unmodified fragment and the corresponding fragment linked to the other peptide.²⁶ A recent systematic study in our laboratory indicated that intermolecularly cross-linked peptides without a mobile proton yielded a high degree of internal ions, as well as other double-cleavage products, which make interpretation of the product ion spectra difficult.³² Thus, developing new chemical cross-linkers to reduce the complexity of the product ion spectra is still an ongoing area of interest. Recent work by Soderblom et al. reported the design of a cross-linker in which a gas-phase labile bond was inserted in the chemical cross-linker, thus cleaving upon

low-energy collisions to yield the two constituent peptides.^{33,34} Bruce and co-workers developed a similar strategy using cross-linkers with two labile bonds that upon dissociation produce the two peptides in addition to a diagnostic reporter fragment ion.^{24,25} After cleavage of the labile bond of these cross-linkers, the two modified peptides are then further interrogated via MS³ to sequence each peptide.

Our aim is to develop a chemical cross-linking technique in conjunction with photodissociation methods to eliminate the need for MSⁿ experiments and streamline the analysis of cross-linked peptides. Infrared multiphoton dissociation (IRMPD) has shown promise as an alternative means to activate and dissociate biomolecules in the gas phase^{35,36} and has been shown to be an effective means to selectively dissociate phosphopeptides in both FTICR^{37,38} and quadrupole ion trap (QIT) mass spectrometers.^{39,40} Previous work in our laboratory³⁹ and by Flora and Muddiman^{37,38,41} have shown that the phosphate group has a high absorption at the wavelength of a continuous wave CO₂ laser, 10.6 μm. Because of the large differences in absorption efficiency of phosphopeptides and unmodified peptides, phosphopeptides dissociate upon IR irradiation far more readily than unmodified peptides.

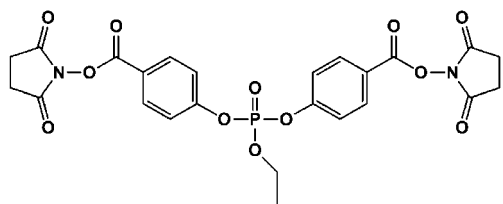
IRMPD in QITs offers other advantages over conventional collisional activation methods.^{36,42–47} IRMPD is a nonresonant activation process whose efficiency is independent of the rf trapping voltage, thus allowing a much broader *m/z* trapping range than conventional CID. This feature is particularly important for detection of key terminal sequence ions in the low *m/z* range. Ion losses due to collisions or unstable trajectories are eliminated as the photodissociation process does not affect the translational motion of ions. The nonresonant nature of photodissociation methods also yields secondary and higher order product ions that might only be obtained by MSⁿ approaches using CID.

In the present study, we have developed a novel IR-chromogenic cross-linker that incorporates a phosphate chromophore that allows the identification of cross-linked peptides and facilitates the interpretation of the product ion spectra of the constituent peptides. IRMPD in a linear quadrupole ion trap is used to selectively dissociate the cross-linked peptides, allowing for these peptides to be easily distinguished from unmodified peptides (i.e., ones that do not afford any protein contact information). The resulting IRMPD spectra of intermolecularly cross-linked peptides

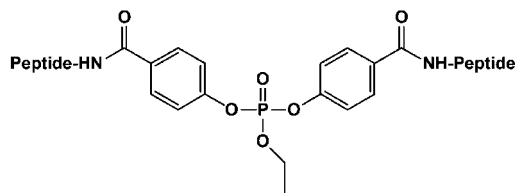
(13) Chu, F.; Mahrus, S.; Craik, C. S.; Burlingame, A. L. *J. Am. Chem. Soc.* **2006**, *128*, 10362–10363.
 (14) Ihling, C.; Schmidt, A.; Kalkhof, S.; Schulz, D. M.; Stingl, C.; Mechtler, K.; Haack, M.; Beck-Sickinger, A. G.; Cooper, D. M. F.; Sinz, A. *J. Am. Soc. Mass Spectrom.* **2006**, *17*, 1100–1113.
 (15) Wine, R. N.; Dial, J. M.; Tomer, K. B.; Borchers, C. H. *Anal. Chem.* **2002**, *74*, 1939–1945.
 (16) Sinz, A.; Wang, K. *Biochemistry* **2001**, *40*, 7903–7913.
 (17) Sinz, A.; Wang, K. *Anal. Biochem.* **2004**, *331*, 27–32.
 (18) Bennett, K. L.; Kussmann, M.; Bjork, P.; Godzwon, M.; Mikkelsen, M.; Sorensen, P.; Roepstorff, P. *Protein Sci.* **2000**, *9*, 1503–1518.
 (19) Petrotchenko, E. V.; Olkhovik, V. K.; Borchers, C. H. *Mol. Cell. Proteomics* **2005**, *4*, 1167–1179.
 (20) Trester-Zedlitz, M.; Kamada, K.; Burley, S. K.; Fenyoe, D.; Chait, B. T.; Muir, T. W. *J. Am. Chem. Soc.* **2003**, *125*, 2416–2425.
 (21) Hurst, G. B.; Lankford, T. K.; Kennel, S. J. *J. Am. Soc. Mass Spectrom.* **2004**, *15*, 832–839.
 (22) Sinz, A.; Kalkhof, S.; Ihling, C. *J. Am. Soc. Mass Spectrom.* **2005**, *16*, 1921–1931.
 (23) Back, J. W.; Hartog, A. F.; Dekker, H. L.; Muijsers, A. O.; de Koning, L. J.; de Jong, L. *J. Am. Soc. Mass Spectrom.* **2001**, *12*, 222–227.
 (24) Tang, X.; Munske, G. R.; Siems, W. F.; Bruce, J. E. *Anal. Chem.* **2005**, *77*, 311–318.
 (25) Chowdhury, S. M.; Munske, G. R.; Tang, X.; Bruce, J. E. *Anal. Chem.* **2006**, *78*, 8183–8193.
 (26) Schilling, B.; Row, R. H.; Gibson, B. W.; Guo, X.; Young, M. M. *J. Am. Soc. Mass Spectrom.* **2003**, *14*, 834–850.
 (27) Gao, Q.; Xue, S.; Doneanu, C. E.; Shaffer, S. A.; Goodlett, D. R.; Nelson, S. D. *Anal. Chem.* **2006**, *78*, 2145–2149.
 (28) Chen, T.; Jaffe, J. D.; Church, G. M. *J. Comput. Biol.* **2001**, *8*, 571–583.
 (29) Tang, Y.; Chen, Y.; Lichti, C. F.; Hall, R. A.; Raney, K. D.; Jennings, S. F. *BMC Bioinformatics* **2005**, *6*, S9.
 (30) de Koning, L. J.; Kasper, P. T.; Back, J. W.; Nessen, M. A.; Vanrobaeys, F.; Van Beeumen, J.; Gherardi, E.; de Koster, C. G.; de Jong, L. *FEBS J.* **2006**, *273*, 281–291.
 (31) Seebacher, J.; Mallick, P.; Zhang, N.; Eddes, J. S.; Aebersold, R.; Gelb, M. H. *J. Proteome Res.* **2006**, *5*, 2270–2282.
 (32) Gardner, M. W.; Brodbelt, J. S. *J. Am. Soc. Mass Spectrom.* **2008**, *19*, 344–357.

(33) Soderblom, E. J.; Bobay, B. G.; Cavanagh, J.; Goshe, M. B. *Rapid Commun. Mass Spectrom.* **2007**, *21*, 3395–3408.
 (34) Soderblom, E. J.; Goshe, M. B. *Anal. Chem.* **2006**, *78*, 8059–8068.
 (35) Little, D. P.; Speir, J. P.; Senko, M. W.; O'Connor, P. B.; McLafferty, F. W. *Anal. Chem.* **1994**, *66*, 2809–2815.
 (36) Payne, A. H.; Glish, G. L. *Anal. Chem.* **2001**, *73*, 3542–3548.
 (37) Flora, J. W.; Muddiman, D. C. *Anal. Chem.* **2001**, *73*, 3305–3311.
 (38) Flora, J. W.; Muddiman, D. C. *J. Am. Chem. Soc.* **2002**, *124*, 6546–6547.
 (39) Crowe, M. C.; Brodbelt, J. S. *J. Am. Soc. Mass Spectrom.* **2004**, *15*, 1581–1592.
 (40) Crowe, M. C.; Brodbelt, J. S. *Anal. Chem.* **2005**, *77*, 5726–5734.
 (41) Flora, J. W.; Muddiman, D. C. *J. Am. Soc. Mass Spectrom.* **2004**, *15*, 121–127.
 (42) Colorado, A.; Shen, J. X.; Brodbelt, J. *Anal. Chem.* **1996**, *68*, 4033–4043.
 (43) Gabryelski, W.; Li, L. *Rapid Commun. Mass Spectrom.* **2002**, *16*, 1805–1811.
 (44) Goolsby, B. J.; Brodbelt, J. S. *Anal. Chem.* **2001**, *73*, 1270–1276.
 (45) Hashimoto, Y.; Hasegawa, H.; Waki, I. *Rapid Commun. Mass Spectrom.* **2004**, *18*, 2255–2259.
 (46) Stephenson, L., Jr.; Booth, M. M.; Shallosky, J. A.; Eyles, J. R.; Yost, R. A. *J. Am. Soc. Mass Spectrom.* **1994**, *5*, 886–893.
 (47) Wilson, J. J.; Brodbelt, J. S. *Anal. Chem.* **2006**, *78*, 6855–6862.

A. IR Chromogenic Crosslinker (IRCX)



B. IRCX crosslink +330 Da



C. IRCX-OH modification +348 Da

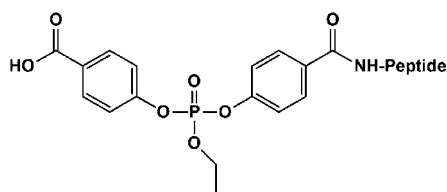


Figure 1. Structures of IRCX (A), an IRCX cross-link (B), and an IRCX-OH modification (C).

are dominated by b- and y-type product ions of each constituent peptide. Online liquid chromatography (LC)-IRMPD-MS has been applied for the screening of complex peptide mixtures, including tryptic digests of chemically cross-linked proteins.

EXPERIMENTAL SECTION

Chemicals and Reagents. The peptides α -MSH (Ac-SYSME-HFRWGKPV-NH₂), Ac-RFMWMK-NH₂, substance P (RPKPQQFF-GLM-NH₂), and neurotensin 1–6 (Pyr-LYENK) were purchased from Bachem (Torrance, CA). The peptide angiotensin II (DRVYI-HPF) was purchased from AnaSpec (San Jose, CA). Ubiquitin from bovine red blood cells, proteomics grade trypsin, bradykinin (RPPGFSPFR), methionine-enkephalin (YGGFM), melittin, and the cross-linker disuccinimidyl suberate (DSS) were obtained from Sigma (St. Louis, MO). *N*-Hydroxysuccinimide, 4-hydroxybenzoic acid, and ethyl dichlorophosphate were from Aldrich (Milwaukee, WI). Water (HPLC grade) and acetonitrile (HPLC grade) were from Riedel-de Haën (Seelze, Germany). 1-Ethyl-3-(3-dimethylaminopropyl)carbodiimide hydrochloride was obtained from Pierce Biotechnology (Rockford, IL). All other chemicals and solvents were purchased from Fisher Scientific (Fairlawn, NJ) except for formic acid (EM Science, Gibbstown, NJ).

Synthesis of Dibenzoyloxysuccinimidyl Ethyl Phosphate.

The IR chromogenic cross-linker (IRCX, Figure 1A), dibenzoyloxysuccinimidyl ethyl phosphate, was synthesized by first preparing the intermediate *N*-(4-hydroxybenzoyloxy)succinimide. Under an argon atmosphere, dry tetrahydrofuran (THF) (45 mL) and dry dichloromethane (DCM) (45 mL) were added to 5 mmol of 4-hydroxybenzoic acid, 8 mmol of *N*-hydroxysuccinimide, and 6.5 mmol of 1-ethyl-3-(3-dimethylaminopropyl)carbodiimide hydrochloride. The reaction was stirred under argon at room temper-

ature for 24 h and then extracted with H₂O (1 × 60 mL), saturated NaHCO₃ (1 × 60 mL), and then a saturated brine solution (1 × 60 mL). The final liquid extract was dried over Na₂SO₄, filtered, and dried under vacuum. The intermediate was recrystallized in DCM at 20 °C overnight and filtered.

Dibenzoyloxysuccinimidyl ethyl phosphate was prepared by dissolving 0.5 mmol of *N*-(4-hydroxybenzoyloxy)succinimide in dry THF at 0 °C and then adding 0.25 mmol of ethyl dichlorophosphate dropwise to the solution, followed by 10 mmol of dry triethylamine. The reaction was allowed to warm to room temperature while stirring over 2 h, and then was heated to 60 °C and stirred for additional 4 h. The final solution was dried and concentrated under reduced pressure. The product was washed with cold H₂O, filtered, recrystallized in DCM, and filtered. The cross-linker structure was confirmed by ¹H NMR using a 400-MHz Varian instrument. ¹H NMR at 400 MHz in CDCl₃ yielded the following: 8.29 (d, 4H), 7.39 (d, 4H), 4.20 (m, 2H), 2.94 (s, 8H), 1.71 ppm (br, 3H); these findings are consistent with the proposed structure. ESI-IRMPD-MS of protonated IRCX (*m/z* 561) using 2.0 ms of irradiation yielded an abundant product ion corresponding to the loss of succinimide (*m/z* 464) and a less abundant ion of *m/z* 446 (loss of *N*-hydroxysuccinimide) (data not shown).

Chemical Cross-Linking of Model Peptides. Stock solutions of the model peptides were prepared at 5.0 mM in H₂O. IRCX and DSS were freshly prepared at 20.0 mM in DMSO prior to cross-linking. The peptides α -MSH and Ac-RFMWMK-NH₂ were intermolecularly cross-linked with IRCX at a 4:4:5 molar ratio of peptide/peptide/cross-linker in 20 mM HEPES, pH 8.0, to produce a final concentration of 1.7 mM in a total volume of 12 μ L. Substance P was similarly intramolecularly cross-linked by IRCX or DSS at a 4:5 molar ratio in the same buffer. All peptide cross-linking reactions were allowed to incubate at room temperature overnight to increase the yield of cross-linked peptides. The reactions were desalted by solid-phase extraction using 50 mg of tC₁₈ Waters (Milford, MA) Sep-Pak cartridges.

Chemical Cross-Linking and Enzymatic Digestion of Ubiquitin. The protein ubiquitin was intramolecularly cross-linked by IRCX at 1:5, 1:10, 1:25, and 1:50 molar ratios of protein/cross-linker in 20 mM HEPES buffer, pH 8.0, at a final protein concentration of 10 μ M. The reactions were allowed to proceed at room temperature for 30 min. The cross-linking was quenched by the addition of NH₄HCO₃ to a final concentration of 10 mM for 15 min. The reaction mixtures were desalted against a 5-kDa molecular mass cutoff Ultrafree Biomax membrane (Millipore, Billerica, MA). Aliquots were removed for direct-ESI-MS analysis, and the remaining cross-linked ubiquitin sample was diluted to 180 μ M in 100 mM NH₄HCO₃, pH 8.0. Cross-linked ubiquitin was enzymatically digested with trypsin at a 1:10 ratio of enzyme to protein (w/w) overnight at 37 °C. The digested sample was then desalted by solid-phase extraction as described above and diluted to ~10 μ M in 50:50 H₂O/MeOH.

Mass Spectrometry and Infrared Multiphoton Dissociation. All mass spectrometry experiments were performed on a modified ThermoFisher LTQ XL linear ion trap mass spectrometer using the XCalibur version 2.2 software package and the standard ESI source. For direct infusion experiments, the ESI voltage was set to 4.5 kV and solutions were infused at 2.5

$\mu\text{L}/\text{min}$. Solutions were prepared at $\sim 10 \mu\text{M}$ in 49.5:49.5:1 $\text{H}_2\text{O}/\text{MeOH}/\text{HOAc}$ (v/v/v) for ESI-MS analysis. For CID experiments, the precursor ions were activated for 30 ms at the default q -value of 0.25. Energy-variable CID experiments were performed by incrementally raising the CID voltage, and the CID voltage necessary to reduce the precursor ion abundance to 50% was determined. For energy-variable CID, normalized collision energies were converted to CID voltages to account for the differences in m/z of the precursor ions based on the calibration settings of the instrument. The CID voltages for the IRCX-cross-linked peptides were then corrected for their greater degrees of freedom compared to the DSS-cross-linked analogues using the following formula:

$$V_{50\%,\text{corrected}} = V_{50\%} \frac{N_{\text{DSS}}}{N_{\text{IRCX}}}$$

where the degrees of freedom $N = 3n - 6$ and n is the number of atoms in the peptide cross-linked by either DSS or IRCX.⁴⁸ All energy-variable CID experiments were performed in triplicate; the drifts in the CID voltages were determined to be less than 0.08 mV.

Infrared Multiphoton Dissociation. IRMPD was performed using a model 48-5 Synrad 50-W CO_2 continuous wave laser (Mukilteo, WA). The back flange of the vacuum manifold of the instrument was modified with a CF viewport flange with a ZnSe window to allow the transmission of 10.6- μm radiation. The unfocused laser beam was aligned on axis with the linear ion trap such that the beam passed through the 2-mm aperture of the exit lens to irradiate the ion cloud. The laser was triggered during the activation step in the scan function by a TTL signal from pin 14 of the J1 connector on the digital printed circuit board. All IRMPD experiments were performed at full power (50 W) with irradiation times varying between 5 and 100 ms unless otherwise indicated. The q -value of the precursor was set between 0.1 and 0.15 to reduce the low-mass cutoff value to less than m/z 150. The pressure in the analyzer region was nominally 9.0×10^{-6} Torr, and no changes to the He bath gas pressure were made.

Analytical High-Performance Liquid Chromatography and Tandem Mass Spectrometry. Liquid chromatography was performed using a Hitachi L-7000 (Hitachi Ltd.) system including an L-7100 HPLC pump and L-7000 autosampler; the LC system was controlled using the Hitachi 3DQ software. Reversed-phase HPLC was accomplished using a Symmetry300 (Waters, Milford, MA) C_{18} column (2.1 \times 50 mm, 3.5- μm packing) with a Symmetry300 C_{18} guard column (2.1 \times 10 mm, 3.5 μm packing). For analytical separations, a gradient elution of mobile phases consisting of (A) H_2O with 0.1% formic acid and (B) acetonitrile with 0.1% formic acid was used at a flow rate of 0.300 mL/min. After loading the sample (10–25- μL injections of 10 μM solutions), the mobile phase was held at 95% A for 2 min and then the peptides were eluted using a linear gradient from 95 to 50% A over 58 min.

Two types of online LC-IRMPD-MS experiments were performed. The first data-acquisition sequence employed the following collection: a full mass spectrum of m/z 300–2000, then an isolation spectrum of m/z 450–2000 in which all ions of m/z in

this range were isolated for 50 ms but not subjected to any form of activation, and then an IRMPD spectrum of all ions of m/z 450–2000 with an irradiation time of 50 ms. For the isolation and IRMPD spectra, the q -value was set to 0.18 for ions of m/z 450, thus establishing the lower m/z limit as 90. The second LC-IRMPD-MS experiment employed data-dependent MS/MS in which IRMPD and CID spectra were acquired for the two most abundant ions observed in the full mass spectrum. IRMPD was performed for 30 ms with the q -value of the precursor ion set to 0.1 (lower m/z limit ranged from 50 to 175 depending on the precursor ion), and CID was performed for 30 ms at a normalized collision energy of 45% using a precursor ion q -value of 0.25 (lower m/z limit 115 – 455).

Identification of Cross-Linked Peptides. Product ion spectra of peptide ions exhibiting high IRMPD efficiency were manually identified aided in part by the software program ProteinXXX, the protein cross-linking function of GPMW (General Protein Mass Analysis for Windows) version 7.10 (Lighthouse Data, Odense, Denmark) (available at <http://www.gpmaw.com>). This program was used to provide a list of intact masses of possible cross-linked tryptic peptides allowing for cleavage C-terminal to only arginine and unmodified lysine residues (i.e., no cleavage C-terminal to cross-linked or dead-end modified lysine residues). The intact mass of the eluting species was matched to the list potential candidates and then the identity of the precursor ion was confirmed manually by IRMPD; all product ions were also identified manually.

RESULTS AND DISCUSSION

Cross-Linker Design and Characterization. It has previously been demonstrated that phosphorylated peptides can be selectively dissociated via IRMPD in a quadrupole ion trap.^{39,40} Our cross-linker (Figure 1A) incorporated a phosphate chromophore due to its greater IR absorption efficiency at 10.6 μm .^{37–39,41} The chromophore was placed in the center of the cross-linker, thus creating a phosphate triester to avoid the neutral loss of phosphoric acid, which is commonly observed upon ion activation of phosphorylated peptides.^{49–52} The cross-linker was designed as a homobifunctional reagent with two terminal NHS-esters that react with primary amines (e.g., ϵ -amine of lysine residues or free N-terminus) similar to most common commercial cross-linkers. IRCX has a spanner arm length of $\sim 16 \text{ \AA}$ and could span a distance up to $\sim 28 \text{ \AA}$ between α -carbons of two lysine residues in proteins. Upon reaction of each NHS-ester with a primary amine, stable amide bonds are formed, yielding a cross-link corresponding to a mass addition of 330 Da (Figure 1B). If one NHS-ester does not react with the protein or peptide and is hydrolyzed, a dead-end modification is produced, termed IRCX-OH as shown in Figure 1C, with a mass addition of 348 Da. Product ions formed upon dissociation of the cross-linked peptides were labeled according to previously suggested nomen-

(48) Jones, J. L.; Dongre, A. R.; Somogyi, A.; Wysocki, V. H. *J. Am. Chem. Soc.* **1994**, *116*, 8368–8369.

(49) Huddleston, M. J.; Annan, R. S.; Bean, M. F.; Carr, S. A. *J. Am. Soc. Mass Spectrom.* **1993**, *4*, 710–717.

(50) Carr, S. A.; Huddleston, M. J.; Annan, R. S. *Anal. Biochem.* **1996**, *239*, 180–192.

(51) DeGnore, J. P.; Qin, J. *J. Am. Soc. Mass Spectrom.* **1998**, *9*, 1175–1188.

(52) Szczepanowska, J.; Zhang, X.; Herring, C. J.; Qin, J.; Korn, E. D.; Brzeska, H. *Proc. Natl. Acad. Sci. U. S. A.* **1997**, *94*, 8503–8508.

clature.^{26,53} Briefly, for intermolecularly cross-linked peptides, the two constituent peptides are labeled α and β , referring to the first and second peptides, respectively. Cleavage along the backbone of the α -peptide yields product ions such as $y_{n\alpha}$ or $b_{n\alpha}$, and similar nomenclature is used for the β -peptide and other product ion types. For intramolecularly cross-linked peptides, the nomenclature is identical to that of unmodified peptides. In addition, lysine immonium ions that are linked to the other peptide are labeled $K^L\alpha$, where L represents the cross-linker and α is the other peptide. Similar nomenclature is used for referring to internal ions of one peptide linked to the second peptide, or a fragment ion of the second peptide (e.g., $b_{4\alpha}^{LY7\beta}$).

IRMPD Analysis of IRCX Cross-Linked Peptides. The peptides α -MSH (α -peptide) and Ac-RFMWMK-NH₂ (β -peptide) were incubated with IRCX, yielding all three possible intermolecularly cross-linked products ($\alpha \otimes \alpha$, $\beta \otimes \beta$, $\alpha \otimes \beta$). The two constituent peptides each have only a single reactive site for the cross-linking reaction, Lys-11 of α -MSH and Lys-6 of Ac-RFMWMK-NH₂ as the N-termini of each of these peptides are acetylated, allowing for the site of the cross-link to be known with certainty for these initial studies. It was possible to readily screen for the cross-linked peptides in the product mixture by acquiring an isolation spectrum in which ions of m/z 400–2000 were isolated for 30 ms without activation by toggling off the isolation waveform, and subsequently acquiring an IRMPD spectrum of ions in the same m/z range by triggering the CO₂ laser for those 30 ms (Figure 2). Upon IR irradiation, only the peptide ions containing an IRCX cross-link or IRCX-OH modification decreased in ion abundance, allowing rapid screening of the IRCX-containing ions of interest. All of the cross-linked peptide ions, regardless of charge state, reduced in ion abundance by more than 95%, as well as the peptide ions with a dead-end IRCX-OH modification. The unmodified peptides did not undergo photodissociation, and no decrease in their ion abundances was observed. After pinpointing the IRCX-cross-linked peptide ions, they can be more closely interrogated by IRMPD, CID, or both. For example, the intermolecularly cross-linked peptide [α -MSH \otimes IRCX \otimes Ac-RFMWMK-NH₂ + 3H]³⁺ was analyzed by IRMPD to determine the location of the cross-link. As shown in Figure 3A, the IRCX-cross-linked peptide underwent very efficient dissociation upon 12 ms of irradiation, and broad sequence coverage of each constituent peptide was observed. CID of the same ion produced similar sequence coverage of each peptide; however, in contrast the triply and doubly charged $b_{11\alpha}$ product ions of m/z 907.5 and 1360.4 dominated the spectrum. Previous work in our laboratory has shown that a proline residue positioned N-terminal to the cross-linked lysine enhances dissociation of the amide bond between the lysine and proline, in this case producing the $b_{11\alpha}$ fragment.³² Most of the product ions observed in the CID spectrum had relative abundances of less than 1%, making it difficult to distinguish these peaks from noise. In addition, due to the limited m/z storage range during CID, the diagnostic $y_{2\alpha}$ product ion of m/z 214.0 cannot be trapped and detected.

Upon closer examination of the IRMPD spectrum in Figure 3A, there is a distinct difference between the relative abundances of the product ions containing the IRCX cross-link and those

without the modification (e.g., $b_{n\alpha}^+$ and $b_{n\beta}^+$ ions). Fragment ions that contain the IRCX cross-link still retain the phosphate chromophore and thus can undergo IR photon absorption and secondary dissociation. CID predominantly yielded product ions that retained the cross-link (e.g., series of $y_{n\alpha}^{2+}$ ions), whereas these fragment ions were less abundant in the IRMPD spectrum. Time-resolved IRMPD was performed in order to investigate the relative abundances of the product ion types observed by varying the irradiation time from 0 to 100 ms. For each IRMPD spectrum acquired, the peak areas of the various product ion types—those containing or not containing the IRCX cross-link—were measured and summed as a function of irradiation time. The time-resolved IRMPD plot in Figure 4 indicates that for irradiation times less than 10 ms the most abundant product ions observed were IRCX-cross-linked fragments. With longer irradiation times, these product ions decreased in relative abundance, forming unmodified b- and y-type ions, and after \sim 30 ms of irradiation, virtually no IRCX-containing product ions survived. Using IRMPD, one can thus circumvent many dead-end dissociation pathways such as dehydration because the primary IRCX-containing fragment ions undergo secondary dissociation to produce more informative fragment ions.

Upon reaction with IRCX, the peptide substance P was intramolecularly cross-linked between the free N-terminus and Lys-3. The doubly protonated IRCX-cross-linked substance P underwent efficient photodissociation using 50 ms of irradiation at only 35 W (Figure 5A). This result, in conjunction with those described above, indicates that both intramolecularly and intermolecularly IRCX-cross-linked peptides can be readily photodissociated. A series of singly charged b-ions were observed along with the dominant y_8 ion, a result of cleavage C-terminal to the intramolecular cross-link, which has previously been noted as a site of enhanced dissociation.⁵³ Collisionally induced dissociation of [substance P \otimes IRCX + 2H]²⁺, as shown in Figure 5B, yielded sequence coverage similar to that of IRMPD, suggesting that either method is suitable for identifying the site of the cross-link. However, in the CID spectrum, the b-ions retaining the IRCX cross-link were observed in both the 1+ and 2+ charge state (e.g., b_8^{2+} , b_9^{2+} , and b_{10}^{2+}), cluttering the product ion spectrum, and fragment ions of low m/z had much lower relative abundances than in the IRMPD spectrum. Upon IR irradiation, the more highly charged IRCX-containing b-ions apparently undergo secondary dissociation at a faster rate than the singly charged ions due to the presence of a mobile proton. In addition, the expanded m/z storage range possible during IRMPD allowed the detection of the low-mass y_1 ion, which was not observed by CID. For precursor ions of higher m/z , the low-mass cutoff inherent to CID would be alleviated by utilizing IRMPD, thus allowing other product ions to be observed that would otherwise be undetectable by CID.

The CID voltages determined from energy-variable CID experiments performed on both DSS- and IRCX-cross-linked peptides indicate the IRCX-cross-linked species have higher dissociation energies than the DSS-cross-linked analogues. For example, for the intermolecularly cross-linked α -MSH and Ac-RFMWMK-NH₂ in the 3+ charge state, the IRCX species had a higher CID voltage than the DSS analogue by 3.7 mV (32.8 versus 29.1 mV). Likewise, the doubly protonated IRCX-intramolecularly

(53) Gaucher, S. P.; Hadi, M. Z.; Young, M. M. *J. Am. Soc. Mass Spectrom.* **2006**, *17*, 395–405.

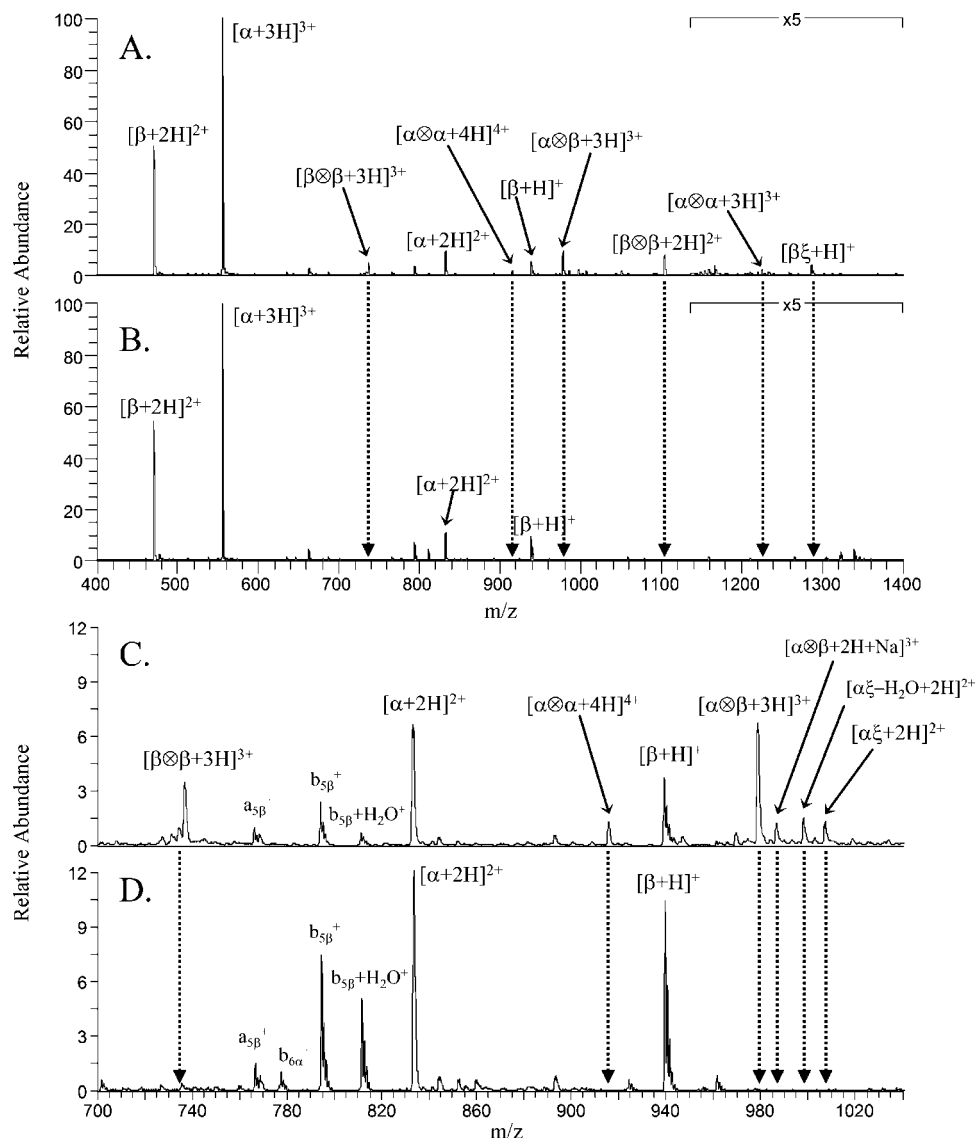


Figure 2. Isolation (A, C) and IRMPD (B, D) spectra of IRCX cross-linking product mixture of α -MSH (α -peptide) and Ac-RFMWMK-NH₂ (β -peptide). IRCX cross-links are represented by \otimes and IRCX-OH dead-end modifications by ξ . Ions were either isolated with the laser off (A, C) or irradiated for 30 ms at 50 W (B, D). Zoomed in region of m/z 700–1040 shown in (C) and (D).

cross-linked substance P required a CID voltage of 1.8 mV greater than that of the analogous DSS-peptide (24.9 versus 23.1 mV). Moreover, the IRCX-containing peptides dissociated readily upon less than 30 ms of irradiation, whereas the DSS-cross-linked peptides did not undergo efficient IRMPD upon irradiation for 250 ms, indicating that the presence of the phosphate chromophore results in a much greater IR absorption at 10.6 μ m (data not shown). These collective results confirm that the successful and selective IRMPD of the IRCX-containing peptides is due to their high IR absorption efficiencies, not due to lower dissociation energies.

Screening of IRCX-Cross-Linked Peptides in a Mock Mixture by IRMPD. IRMPD analysis was performed on a mock mixture of peptides to demonstrate selective dissociation of IRCX-cross-linked peptides. The peptide mixture contained an equimolar amount (10 μ M) of Pyr-LYENK (1), YGGFM (2), bradykinin (3), angiotensin II (4), α -MSH (5), Ac-RFMWMK-NH₂ (6), substance P (7), and melittin (13). Also present were equimolar amounts

(10 μ M) of the IRCX intermolecular cross-linked product mixture of α -MSH with Ac-RFMWMK-NH₂ and the intramolecular cross-linked product mixture of substance P. Products observed in the ESI mass spectrum included α -MSH + IRCX-OH (8), α -MSH \otimes IRCX \otimes α -MSH (9), substance P \otimes IRCX (10), α -MSH \otimes IRCX \otimes Ac-RFMWMK-NH₂ (11), and Ac-RFMWMK-NH₂ \otimes IRCX \otimes Ac-RFMWMK-NH₂ (12). Using direct infusion ESI-MS, the mixture was rapidly screened by comparing the abundances of ions of m/z 450–2000 in the isolation spectrum (Supporting Information, Figure 1A) to the IRMPD spectrum obtained using 25 ms of irradiation at 50 W (Supporting Information, Figure 1B). The abundances of the unmodified peptide ions are unaffected by IR irradiation, whereas the IRCX-cross-linked peptide ions readily photodissociate with reductions in ion abundance of \sim 90% with the exception of the singly protonated intramolecularly cross-linked substance P ion (Supporting Information, Table 1). While the doubly charged analogue undergoes efficient IRMPD, the singly protonated species, which does not have a mobile proton,

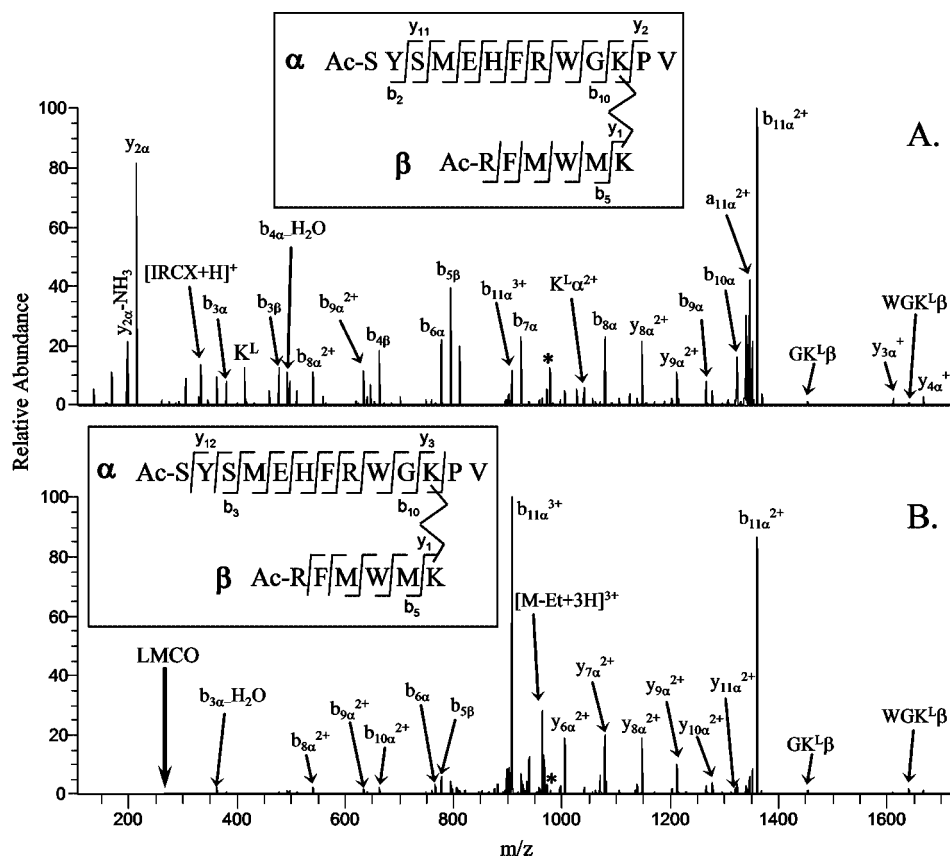


Figure 3. Product ion spectra of $[\alpha\text{-MSH} \otimes \text{IRCX} \otimes \text{Ac-RFMWMK-NH}_2 + 3\text{H}]^{3+}$ (A) IRMPD of m/z 978.5 ($q = 0.1$, 12 ms, 50 W) and (B) CID of m/z 978.5 ($q = 0.25$, 30 ms, 34.1 mV). α -MSH is referred to as the α -peptide and Ac-RFMWMK-NH₂ as the β -peptide. The precursor ion is represented by an asterisk (*).

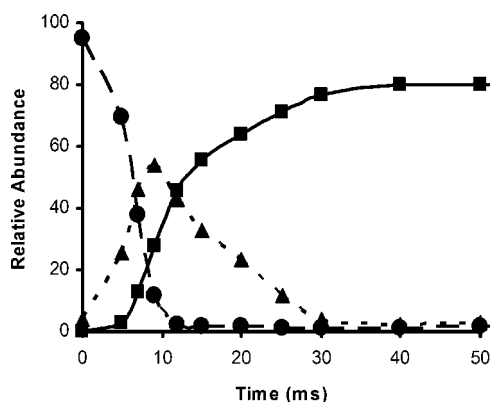


Figure 4. Time-resolved IRMPD (50 W) of $[\alpha\text{-MSH} \otimes \text{IRCX} \otimes \text{Ac-RFMWMK-NH}_2 + 3\text{H}]^{3+}$ displaying the relative abundances of the precursor ion (●), non-IRCX-containing product ions (■), and IRCX containing product ions (▲). Ion abundances are all relative to the total ion abundance of the spectrum acquired with 0 ms of irradiation.

actually increased in abundance upon IR irradiation in this experiment (relative abundance increased from 0.39 to 0.51%). This charge-state dependence on IRMPD efficiencies provides a means to distinguish between intra- and intermolecularly IRCX cross-linked peptides, in which the intermolecularly cross-linked peptides of all charge states exhibit high photodissociation efficiencies. Most intramolecularly cross-linked tryptic peptides will possess a free N-terminus and either an unmodified Lys or Arg at the C-terminus and thus will predominantly be observed as

doubly charged ions, leading to efficient IRMPD. No discernible decrease in the ion abundances of the unmodified peptides was observed using irradiation times of greater than 250 ms; this indicates that the laser irradiation time and power has an ample range of usability to differentiate between IRCX-cross-linked peptides and unmodified ones.

For more complex mixtures such as those expected for peptides with isobaric m/z values, an HPLC separation is required prior to IRMPD screening, as demonstrated for the same mock mixture. As detailed in the Experimental Section, the scan sequence to accomplish this task includes acquisition of a full mass spectrum, then an isolation mass spectrum from m/z 450 to 2000, and then an IRMPD mass spectrum of all isolated ions. Selected ion chromatograms (SICs) for each of the species in the mixture were extracted and then plotted together to form a reconstructed ion chromatogram (RIC). The reconstructed ion chromatograms for the isolation and IRMPD spectra are shown in Figure 6, and the changes in ion abundances are summarized in Table 1. The difference between the RICs for the isolation and IRMPD mass spectra is striking. Upon IR irradiation, the unmodified peptide ions did not exhibit any decrease in ion abundance with the exception of $[\text{melittin} + 5\text{H}]^{5+}$, which decreased in abundance by $\sim 20\%$ (based on peak areas in the SICs). In contrast, the IRCX-cross-linked and modified peptide ions are reduced on the order of 60–100% in abundance after irradiation. All of the species that eluted between 37 and 44 min contained either an IRCX cross-link or an IRCX-OH modification, and upon 25 ms of IR irradiation,

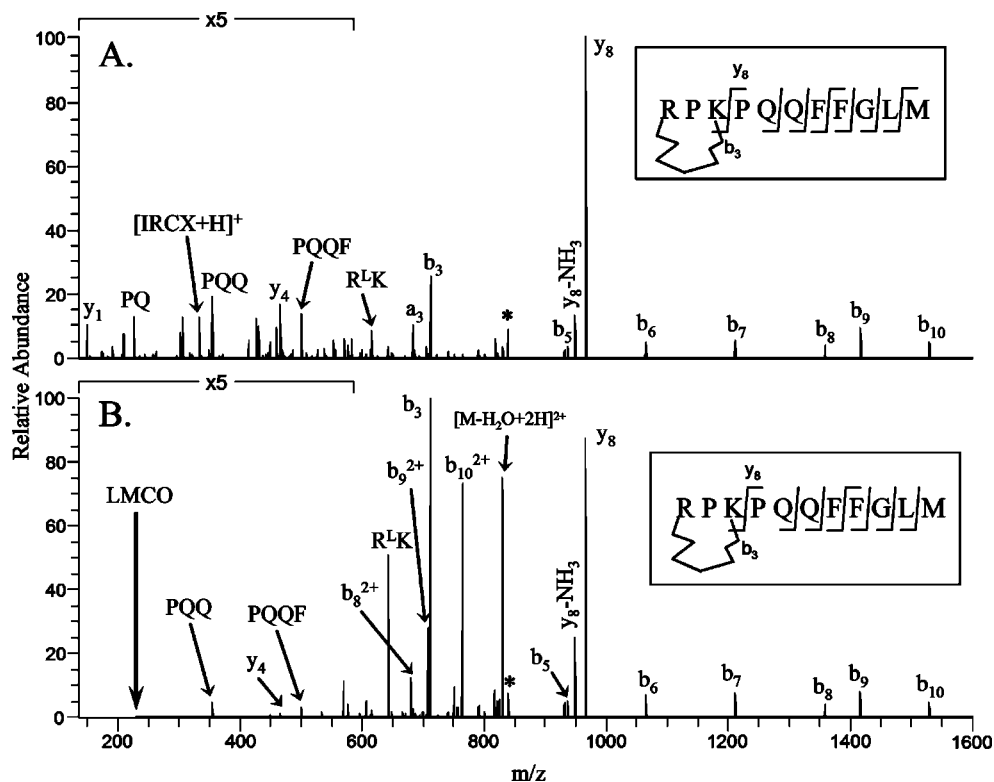


Figure 5. Product ion spectra of $[\text{substance P} \otimes \text{IRCX} + 2\text{H}]^{2+}$ (A) IRMPD of m/z 839.3 ($q = 0.15$, 50 ms, 35 W) and (B) CID of m/z 839.3 ($q = 0.25$, 30 ms, 26.7 mV). The precursor ion is represented by an asterisk (*).

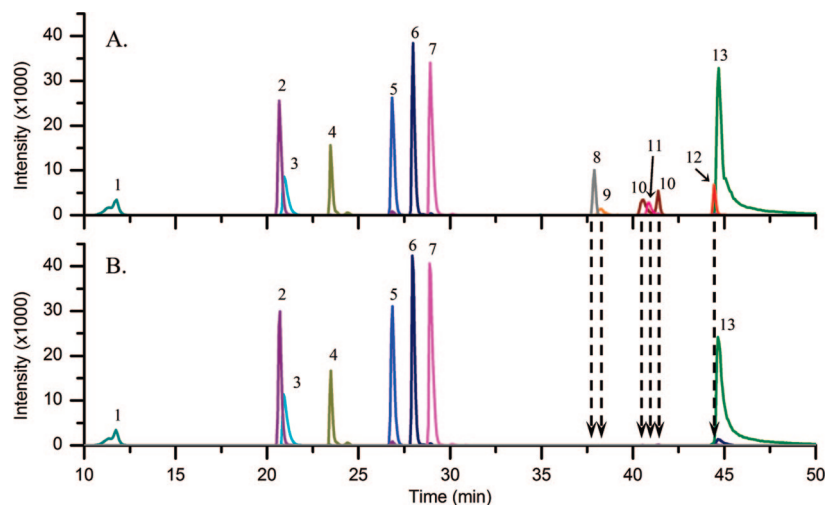


Figure 6. Reconstructed ion chromatograms of (A) isolation (25 ms) and (B) IRMPD (25 ms, 50 W) spectra from LC-IRMPD-MS of a mock mixture of peptides. The identities of the eluting species are listed in Table 2. Ion chromatogram intensities of $[\alpha\text{-MSH} + \text{IRCX-OH} + 2\text{H}]^{2+}$ (**8**) and $[\alpha\text{-MSH} \otimes \text{IRCX} \otimes \alpha\text{-MSH} + 4\text{H}]^{4+}$ (**9**) were zoomed in 10 \times in both (A) and (B).

the intact peptide ions containing the IRCX chromophore were no longer detected.

LC-IRMPD-MS of IRCX Cross-Linked Ubiquitin. To test the utility of LC-IRMPD-MS for screening and identifying IRCX-cross-linked peptides, a trypsin digest of IRCX-cross-linked ubiquitin was analyzed as a model cross-linked protein. Upon incubation with IRCX, ESI-MS analysis indicated that ubiquitin was modified to different degrees. For the lowest molar ratio of cross-linker to protein (5:1), the most abundant species present was unmodified ubiquitin; also observed at approximately the same abundance in the ESI mass spectrum was ubiquitin with a single

dead-end modification as well as singly cross-linked ubiquitin. At a 25:1 molar ratio, upward of two modifications were observed but the singly cross-linked species was the most abundant. Unmodified ubiquitin was still detected as the least abundant species. The most abundant species observed in the full mass spectrum of 50:1 IRCX-cross-linked ubiquitin corresponded to the introduction of a single cross-link and a single dead-end modification (Supporting Information, Figure 2). Also observed, but to lesser degrees, was ubiquitin with two IRCX cross-links, as well as ubiquitin possessing three total modifications (combination of two cross-links and one dead-end modification or one cross-link

Table 1. Decreases in Ion Abundance upon IR Irradiation from LC-IRMPD-MS Reconstructed Ion Chromatograms of a Mock Mixture of Peptides^a

label	elution (min)	species	<i>m/z</i>	peak area isolation	peak area IRMPD	percent abundance decrease
1	11.8	[Pyr-LYENK + H] ⁺	777.4	2072.76	1853.80	10.6
2	20.7	[YGGFM + H] ⁺	574.2	5402.80	6251.49	-15.7
3	20.9	[bradykinin + 2H] ²⁺	530.7	2942.05	3595.30	-22.2
4	20.9	[bradykinin + H] ⁺	1060.5	49.78	53.84	-8.2
	23.5	[angiotensin II + 2H] ²⁺	523.8	2806.80	3087.37	-10.0
5	23.5	[angiotensin II + H] ⁺	1046.5	131.89	122.36	7.2
	26.8	[α-MSH + 3H] ³⁺	555.6	5863.15	6994.73	-19.3
6	26.8	[α-MSH + 2H] ²⁺	832.9	1533.24	1717.75	-12.0
	26.8	[α-MSH + H] ⁺	1664.8	5.28	7.12	-35.0
	28.0	[Ac-RFMWMK-NH ₂ + 2H] ²⁺	470.2	7154.23	8144.27	-13.8
7	28.0	[Ac-RFMWMK-NH ₂ + H] ⁺	939.5	181.80	168.69	7.2
	28.9	[substance P + 2H] ²⁺	674.4	7937.77	9496.41	-19.6
8	28.9	[substance P + H] ⁺	1347.7	179.17	189.83	-5.9
	37.9	[α-MSH + IRCX-OH + 2H] ²⁺	1006.9	190.39	0.00	100.0
9	38.3	[α-MSH ⊗ IRCX ⊗ α-MSH + 4H] ⁴⁺	915.4	53.83	0.00	100.0
	28.3	[α-MSH ⊗ IRCX ⊗ α-MSH + 3H] ³⁺	1220.2	7.89	0.06	99.2
10	40.6, 41.4	[substance P ⊗ IRCX + 2H] ²⁺	839.4	2459.99	0.06	100.0
	40.6, 41.4	[substance P ⊗ IRCX + H] ⁺	1677.7	77.85	31.29	59.8
11	40.9	[α-MSH ⊗ IRCX ⊗ Ac-RFMWMK-NH ₂ + 3H] ³⁺	978.4	894.07	0.00	100.0
	40.9	[α-MSH ⊗ IRCX ⊗ Ac-RFMWMK-NH ₂ + 2H] ²⁺	1467.1	69.18	12.89	81.4
	44.4	[2(Ac-RFMWMK-NH ₂) ⊗ IRCX + 3H] ³⁺	736.6	218.90	11.68	94.7
12	44.4	[2(Ac-RFMWMK-NH ₂) ⊗ IRCX + 2H] ²⁺	1104.5	1165.07	12.79	98.9
13	44.7	[melittin + 5H] ⁵⁺	570.1	19847.59	16037.27	19.2
	44.7	[melittin + 4H] ⁴⁺	712.4	18792.54	19778.43	-5.2
	44.7	[melittin + 3H] ³⁺	949.6	4885.16	5050.55	-3.4

^a Percent abundance decreases calculated from the decrease of the peak areas of the SICs from the isolation and IRMPD spectra.

Table 2. Decreases in Ion Abundance upon IR Irradiation from LC-IRMPD-MS Reconstructed Ion Chromatograms of a Tryptic Digest of Ubiquitin Cross-Linked by IRCX

label	elution (min)	species	<i>m/z</i>	primary sequence ^b	average % abundance decrease ^c	std dev ^c
1	0.6	[30-42] ³⁺	509.0	IQDKEGIPPDQQR	31	14
2	15.5	[55-63] ²⁺	541.3	TLSDYNIQK	-28	4
3	16.6	[43-48] ⁺	648.3	LIFAGK	-4	5
4	22.0	[64-72] ²⁺	534.6	ESTLHLVLR	-28	17
5	26.0	[12-27] ²⁺	894.6	TITLEVEPSDTIENVK	-37	15
6	27.0	[55-72] ³⁺	710.8	TLSDYNIQK*ESTLHLVLR	-66	24
7	31.6, 33.2	[30-42 ⊗ IRCX ⊗ 7-27] ⁴⁺	1036.1	IQDK*EGIPPDQQR ⊗ IRCX ⊗ TLTGK*TITLEVEPSDTIENVK	100.0	0.0
8	32.8, 35.4	[43-54 + IRCX-OH] ²⁺	848.0	LIFAGK*QLEDGR + IRCX-OH	100.0	0.0
9	33.1	[55-72 ⊗ IRCX + 30-42] ⁵⁺	797.8	TLSDYNIQK*ESTLHLVLR + IRCX + IQDK*EGIPPDQQR	100.0	0.0
	33.1	[55-72 ⊗ IRCX ⊗ 30-42] ⁴⁺	996.6	TLSDYNIQK*ESTLHLVLR ⊗ IRCX ⊗ IQDK*EGIPPDQQR	100.0	0.0
10	35.3, 37.6	[1-11 + IRCX-OH] ²⁺	807.0	MQIFVK*TLTGK + IRCX-OH	99	1
11	36.0, 37.9	[55-72 + IRCX-OH] ³⁺	826.8	TLSDYNIQK*ESTLHLVLR + IRCX-OH	100.0	0.0
12	37.0	[55-72 ⊗ IRCX ⊗ 43-54] ⁵⁺	762.9	TLSDYNIQK*ESTLHLVLR ⊗ IRCX ⊗ LIFAGK*QLEDGR	100.0	0.0
	37.0	[55-72 ⊗ IRCX ⊗ 43-54] ⁴⁺	952.8	TLSDYNIQK*ESTLHLVLR ⊗ IRCX ⊗ LIFAGK*QLEDGR	92	5
	37.0	[55-72 ⊗ IRCX ⊗ 43-54] ³⁺	1269.6	TLSDYNIQK*ESTLHLVLR ⊗ IRCX ⊗ LIFAGK*QLEDGR	99.4	0.8
13	37.8	[55-72 ⊗ IRCX ⊗ 1-11] ⁵⁺	746.9	TLSDYNIQK*ESTLHLVLR ⊗ IRCX ⊗ MQIFVK*TLTGK	100.0	0.0
	37.8	[55-72 ⊗ IRCX ⊗ 1-11] ⁴⁺	932.7	TLSDYNIQK*ESTLHLVLR ⊗ IRCX ⊗ MQIFVK*TLTGK	99.9	0.1

^a Percent abundance decreases calculated from the decrease of the peak areas of the SICs from the isolation and IRMPD spectra. ^b Site of modification or cross-link represented by *. ^c Standard deviation of the percent abundance decreases obtained in triplicate.

and two dead-end modifications). All LC-IRMPD-MS analyses were performed on the product mixture of the 50:1 molar ratio of IRCX to ubiquitin to eliminate any unmodified ubiquitin from the sample. No separation of the different IRCX cross-linked and modified ubiquitin products was performed, and all products were subjected simultaneously to trypsin digestion. After digestion, the tryptic peptides were separated and analyzed by LC-IRMPD-MS in a manner similar to the mock mixture described above, acquiring isolation and IRMPD spectra of ions of *m/z* 450–2000. The RICs for the isolation spectra and IRMPD spectra are shown in Figure

7, and the eluting species are summarized in Table 2. The differences between the two chromatograms are dramatic—only the IRCX-cross-linked or modified peptides (species labeled 7–13) exhibit IRMPD, and upon 50 ms of irradiation decrease in ion abundance to below the detection limit. On average, the unmodified peptide ions exhibited an increase in ion abundance of ~20%, which we attribute to fluctuations in ion trapping during the isolation and IRMPD steps, as well as to differences in the number of ions being injected into the trap between the two scans, despite using the automatic gain control feature of the ion trap. The IRCX-

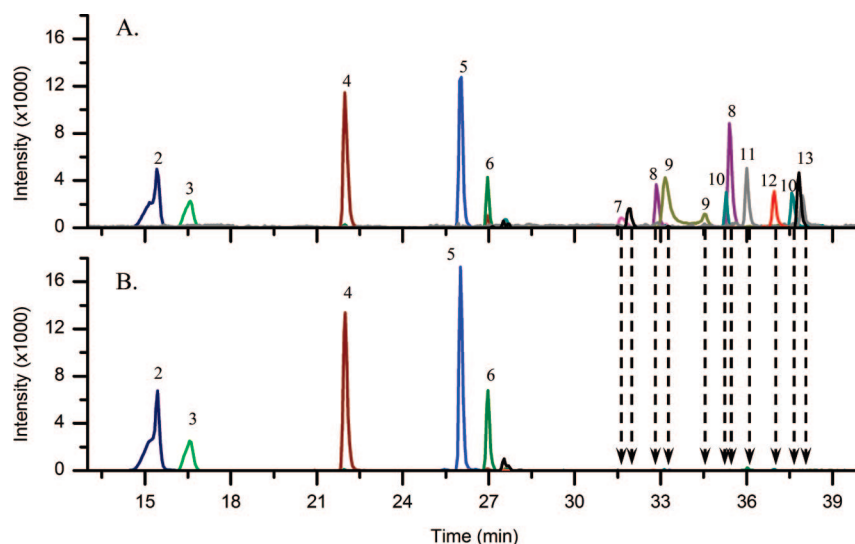


Figure 7. Reconstructed ion chromatograms of (A) isolation (50 ms) and (B) IRMPD (50 ms, 50 W) spectra from LC-IRMPD-MS of a tryptic digest of ubiquitin cross-linked by IRCX. See Table 3 for identities of eluting species. Ion chromatogram intensities of $[43-48]^+$ (**3**), $[55-72]^{3+}$ (**6**), $[30-42 \otimes \text{IRCX} \otimes 7-27]^{4+}$ (**7**), $[55-72 \otimes \text{IRCX} \otimes 30-42]^{5+}$ (**9**), $[1-11 + \text{IRCX-OH}]^{2+}$ (**10**), $[55-72 + \text{IRCX-OH}]^{3+}$ (**11**), and $[55-72 \otimes \text{IRCX} \otimes 1-11]^{5+}$ (**13**) were zoomed in by $10\times$ in both (A) and (B).

Table 3. Summary of Cross-Links and Modifications of Ubiquitin Identified Using IRCX and LC-IRMPD-MS

tryptic fragment	peptide sequence(s) ^a	complex mass measured ^b	complex mass calculated ^b	charge states observed	cross-linked/modified site(s)	distance (Å) ^c	intensity ^d
30-42	IQDK*EGIPPDQQR	4140.4	4140.0	4+	Lys-33	13.3	0.5
7-27	TLTGK*TITLVEPSDTIENVK				Lys-11		
55-72	TLSDYNIQK*ESTLHLVLR	3982.8	3982.0	5+, 4+	Lys-63	19.6	151.3
30-42	IQDK*EGIPPDQQR				Lys-33		
55-72	TLSDYNIQK*ESTLHLVLR	3805.7	3804.9	5+, 4+, 3+	Lys-63	18.4	1421.0
43-54	LIFAGIK*QLEDGR				Lys-48		
55-72	TLSDYNIQK*ESTLHLVLR	3724.9	3723.9	5+, 4+	Lys-63	15.1	177.3
1-11	MQIFVK*TLTGK				Lys-6		
43-54	LIFAGIK*QLEDGR	1693.8	1694.8	2+	Lys-48	n/a	3067.1
1-11	MQIFVK*TLTGK	1613.3	1613.8	2+	Lys-6	n/a	226.8

^a Site of modification or cross-link represented by *. ^b Neutral monoisotopic mass in Da. ^c Distance between α -carbons of lysine residues calculated from X-ray crystal structure of ubiquitin (PDB: 1AAR). ^d Total ion current in counts from full MS scans in isolation/IRMPD LC-IRMPD-MS experiment.

cross-linked peptides decreased by $\sim 100\%$, with the exception of $[\text{T}^{55}\text{LSDYNIQK}^{63}\text{ESTLHLVLR}^{72} \otimes \text{IRCX} \otimes \text{L}^{43}\text{IFAGIK}^{48}\text{QLEDGR}^{54} + 4\text{H}]^{4+}$, which was reduced in abundance by 92%. The abundance of this quadruply charged cross-linked peptide likely did not decrease by 100% due to an isobar with the $y_{10\beta} 17^{3+}$ product ion, corresponding to cleavage C-terminal to the cross-linked Lys-48 of $\text{L}^{43}\text{IFAGIK}^{48}\text{QLEDGR}^{54}$ and incomplete secondary dissociation of this fragment ion. Even with this isobaric overlap, there is a consistent difference in IRMPD efficiencies that allows the IRCX-cross-linked peptides to be readily distinguished.

While comparing isolation and IRMPD spectra to determine which peptide ions undergo photodissociation upon IR irradiation allows rapid pinpointing of the IRCX-cross-linked peptides, one cannot directly use these IRMPD spectra to locate the site of cross-linking because all ions of m/z 450–2000 are irradiated simultaneously in the screening step, creating complicated, overlapping dissociation patterns of all IRCX-cross-linked peptides. In order to obtain product ion information of individual cross-linked peptides, data-dependent MS/MS was utilized to isolate and subsequently perform IRMPD on the most abundant ions.

None of the unmodified tryptic peptides of ubiquitin underwent IRMPD, again allowing for them to be distinguished from the IRCX-cross-linked peptides. An example of an IRMPD mass spectrum of an unmodified peptide is shown in Supporting Information, Figure 3A, in which doubly protonated $\text{T}^{12}\text{ITLVEPSDTIENVK}^{27}$ does not photodissociate upon 30 ms of IR irradiation; the precursor ion remains the only ion observed in the spectrum. In contrast, IRMPD spectra acquired during the data-dependent LC-IRMPD-MS method for three IRCX-cross-linked peptides are shown in Figure 8, and in all cases, the precursor ions readily photodissociate. For example, the second cross-linked peptide to elute contains $\text{T}^{55}\text{LSDYNIQK}^{63}\text{ESTLHLVLR}^{72}$ (α -peptide) linked to $\text{I}^{30}\text{QDK}^{33}\text{EGIPPDQQR}^{42}$ (β -peptide) through Lys-63 and Lys-33. IRMPD of this cross-linked peptide ion provided 10 unique sequence ions (Figure 8A). No product ions containing the IRCX cross-link were observed, most likely a result of secondary dissociation of these fragment ions. Almost a full series of y_{α} ions without the IRCX cross-link (e.g., y_{α} ions C-terminal of the cross-linked Lys-63) were detected, providing a sequence tag for identifying one of the two constituent

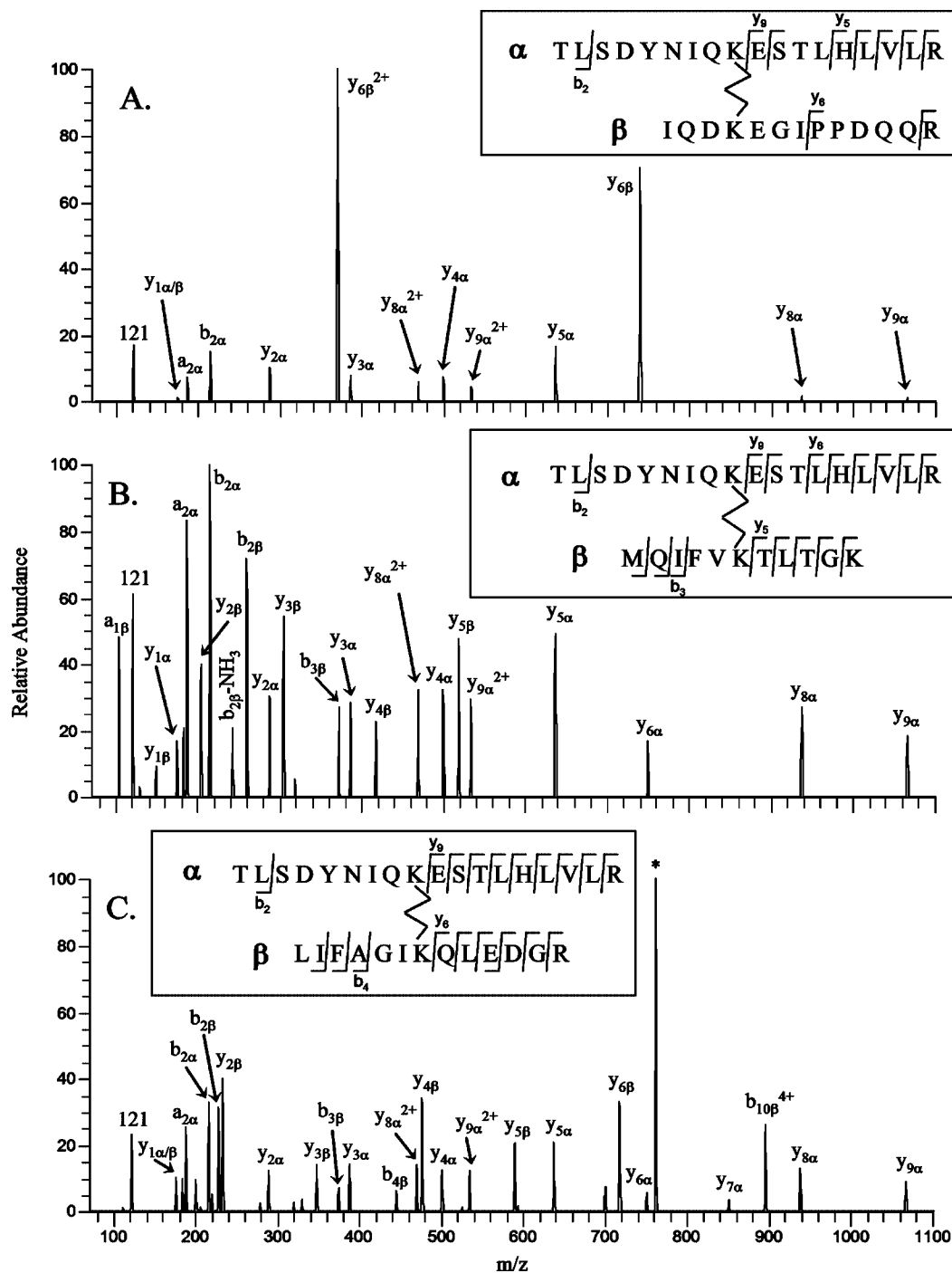


Figure 8. IRMPD spectra (30 ms, 50 W, $q = 0.1$) of tryptic peptides of ubiquitin cross-linked by IRCX acquired during data-dependent LC-IRMPD-MS experiment: (A) $[T^{55}LSDYNIQK^{63}ESTLHHLVLR^{72} \otimes IRCX \otimes I^{30}QDK^{33}EGIPPDQQR^{42} + 5H]^{5+}$ of m/z 797.8, (B) $[T^{55}LSDYNIQK^{63}ESTLHHLVLR^{72} \otimes IRCX \otimes M^1QIFVK^6TLTGK^{11} + 5H]^{5+}$ of m/z 746.1, and (C) $[T^{55}LSDYNIQK^{63}ESTLHHLVLR^{72} \otimes IRCX \otimes L^{43}IFAGIK^{48}QLEDGR^{54} + 5H]^{5+}$ of m/z 762.4. The first peptide listed is the α -peptide; the second peptide is referred to as the β -peptide. Lysine residues in boldface font indicate the site of the cross-link. Precursor ions, if observed, are labeled with an asterisk (*).

peptides. The highly abundant $y_{6\beta}$ ions, result of cleavage N-terminal to Pro-37, provide information necessary to determine that the β -peptide contains P³⁷PDQQR⁴². However, the corresponding $b_{7\beta}$ product ion, which contains the chromophore and the α -peptide, can undergo secondary dissociation to yield additional diagnostic fragment ions. Along with the identity of the α -peptide and the intact mass of the cross-linked peptide, one can deduce the identity of the second peptide and finally the location of the cross-link, between Lys-63 and Lys-33. In contrast, CID of

the 5+ charge state of this cross-linked peptide yielded only seven identifiable product ions ($y_{6\beta}^{2+}$, $y_{6\beta}^+$, $y_{8\alpha}^{2+}$, $y_{4\beta}^+$, $y_{8\beta}^+$, $y_{16\alpha}^{4+}$, $b_{7\beta}^{3+}$), three of which correspond to cleavage N-terminal to Pro-37 (Supporting Information, Figure 3B). No sequential series of product ions was observed using CID, and most of the ions observed could not be identified as typical a-, b-, or y-type ions (including double-cleavage products). The IRCX-cross-linked peptide containing T⁵⁵LSDYNIQK⁶³ESTLHHLVLR⁷² (α -peptide) and

M¹QIFVK⁹TLTGK¹¹ (β -peptide) readily photodissociated upon IR irradiation, yielding only fragment ions without the IRCX chromophore (Figure 8B). Thirteen of the 14 amide bonds C-terminal to the cross-linked lysines were cleaved by IRMPD, providing a sequence tag for both constituent peptides. CID of this cross-linked peptide yielded a variety of product ions including both b- and y-type fragment ions with and without the cross-link (Supporting Information, Figure 3C). In addition several double-cleavage product ions were observed including a series of $y_{16\alpha}^1 y_{n\beta}$ ions (i.e., $y_{16\alpha}$ fragment linked to a y-ion of the β -peptide), which complicate interpretation of the CID spectrum. IRMPD alone provides far more diagnostic product ions allowing for the cross-linked peptide to be identified. For the cross-linked peptide ion [T⁵⁵LSDYNIQK⁶³ESTLHLVLR⁷² \otimes IRCX \otimes L⁴³IFAGK⁴⁸-QLEDGR⁵⁴ + 5H]⁵⁺, all of y-ions C-terminal to the two cross-linked lysine residues were detected using IRMPD (Figure 8C). Using these y-ions, one could easily sequence the C-terminal ends of the two constituent peptides via a de novo approach. In addition, three $b_{n\beta}$ product ions were detected providing confirmation of the identity of the β -peptide, L⁴³IFAGIK⁴⁸QLEDGR⁵⁴. Two dead-end modifications, at Lys-48 and Lys-6, could also be identified. The IRMPD mass spectrum for the species containing L⁴³IFAGIK⁴⁸QLEDGR⁵⁴ modified by IRCX-OH at Lys-48 is shown in Supporting Information, Figure 3D. Cleavage of all backbone amide bonds occurred, yielding a series of b-ions N-terminal to the modified lysine and a series of y-ions C-terminal to the modified lysine, all without the IRCX chromophore.

A majority of the product ions observed upon IRMPD were y-ions without the IRCX cross-link, as opposed to b-ions. Earlier work in our laboratory suggested that there is a preference for cleavage C-terminal to the cross-linked lysine for intermolecularly cross-linked peptides, possibly due to charge localization on the C-terminal arginine residues.³² Dissociation at this amide bond of the α -peptide would result in a y_{α} -ion with a protonated C-terminal arginine and a b_{α} -ion retaining the IRCX cross-link and the β -peptide. This b_{α} -ion would likely undergo secondary and higher order dissociation since it contains the phosphate chromophore, possibly producing an un-cross-linked y_{β} -ion. Any secondary product ion still retaining the chromophore may continue to absorb photons and dissociate, resulting in small fragments that are not observed (e.g., neutral fragments, m/z below the low-mass cutoff, etc.). However, if a charge is retained on the N-terminus, un-cross-linked b-ions would also be detected.

In all of the IRMPD mass spectra of the IRCX-cross-linked and IRCX-OH modified peptides, a product ion of m/z 121 was detected. This fragment ion, observed only after significant secondary dissociation, corresponds in mass to a double-cleavage product—cleavage of the cross-link amide bond and between the P–O bond nearest the cleaved amide bond. The formation of this diagnostic product ion, which is not isobaric with any immonium ions of the amino acids, provides another means of distinguishing IRCX-cross-linked peptides from unmodified ones. Using traditional CID, one would not observe this reporter ion as it has an m/z value below the low-mass cutoff. Moreover, as a higher-order product ion, it is only observed after significant secondary dissociation afforded by IRMPD, not CID.

In total, four cross-links and two dead-end modifications were identified using the IRCX and LC-IRMPD-MS strategy, as sum-

marized in Table 3. IRCX has a spacer arm length of ~ 16 Å, and given the flexibility of lysine side chains, distances of ~ 28 Å between α -carbons of lysines could be spanned. For all four of the observed cross-links, the distance between the α -carbons was less than 20 Å based on the X-ray crystal structure (PDB: 1AAR). The two phenyl groups of IRCX create a more rigid cross-linker that may not be able to easily span short distances, as evident by the fact that no cross-links spanning a distance of less than 13 Å were observed. The rigidity of IRCX would not promote the formation of short cross-links as the one observed between Lys-6 and Lys-11 ($\Delta x = 5.8$ Å) in a previous study using DSS.⁵⁴ Three of the four cross-links identified in the present study involved Lys-63, which is located on the surface of ubiquitin. Upon creation of an amide bond between IRCX and Lys-63, the other NHS-ester of IRCX could react with other surface-accessible lysines within 20 Å, including Lys-48, Lys-33, and Lys-6, yielding a mixture of cross-linked products, as observed. While other lysines are potential sites of cross-linking, Lys-63 is likely more reactive resulting in limited structural information. Recently, a partial acetylation technique has been used to enhance the diversity of cross-linking reactions by blocking the more reactive lysine residues to provide more comprehensive distance constraints.⁵⁵ Using such an approach may yield more informative cross-links between other lysine pairs. The two dead-end modifications were located at Lys-48 and Lys-6, two other surface-accessible primary amines that were also observed to be cross-linked.

CONCLUSIONS

By incorporating a phosphate chromophore into our chemical cross-linker IRCX, we have shown that both intra- and intermolecularly cross-linked peptides can be rapidly distinguished from unmodified peptides using IRMPD-MS. Using 50 ms of irradiation, only the IRCX cross-linked or dead-end modified peptides underwent efficient photodissociation, thus allowing the identification of these key species by simply comparing ion abundances before and after exposure to IR irradiation. This technique has been successfully applied to both direct-infusion ESI-IRMPD-MS and online LC-IRMPD-MS using data-dependent MS/MS experiments for a mock mixture of peptides and a tryptic digest of IRCX-cross-linked ubiquitin. For the cross-linked ubiquitin sample, a total of four cross-links and two dead-end modifications were observed, and the locations of the cross-links were unambiguously identified. IRMPD of the intermolecularly cross-linked peptides yielded a series of y-ions C-terminal to the cross-linked lysines without the IRCX cross-link due to secondary dissociation of fragment ions containing the chromophore. These product ions could then be used to sequence each of the two constituent peptides in a de novo manner, potentially providing a ready means to identify not only the cross-linked peptides but also the proteins in an intracellular chemical cross-linking experiment.

ACKNOWLEDGMENT

Funding from the Welch Foundation (F1155) and the National Science Foundation (CHE-0718320) is gratefully acknowledged.

(54) Kruppa, G. H.; Schoeniger, J.; Young, M. M. *Rapid Commun. Mass Spectrom.* **2003**, *17*, 155–162.

(55) Guo, X.; Bandyopadhyay, P.; Schilling, B.; Young, M. M.; Fujii, N.; Aynechi, T.; Guy, R. K.; Kuntz, I. D.; Gibson, B. W. *Anal. Chem.* **2008**, *80*, 951–960.

ThermoFisher is also gratefully acknowledged for their assistance in the modification of the instrument control files.

SUPPORTING INFORMATION AVAILABLE

Figure 1, isolation and IRMPD spectra of a mock mixture of peptides; Figure 2, deconvoluted and full ESI-MS of IRCX cross-linked ubiquitin; Figure 3, product ion spectra of tryptic peptides of IRCX cross-linked ubiquitin including IRMPD of [12–27]²⁺, CID of [55–72 ⊗ IRCX ⊗ 30–42]⁵⁺, CID of [55–72 ⊗ IRCX ⊗

1–11]⁵⁺, and IRMPD of [43–54 + IRCX-OH]²⁺; Table 1, relative ion abundance decreases upon IR irradiation for the mock mixture of peptides. This material is available free of charge via the Internet at <http://pubs.acs.org>.

Received for review March 27, 2008. Accepted May 13, 2008.

AC800625X